



Study on morphology of high-aspect-ratio grooves fabricated by using femtosecond laser irradiation and wet etching

Tao Chen^a, An Pan^a, Cunxia Li^b, Jinhai Si^{a,*}, Xun Hou^a

^a Key Laboratory for Physical Electronics and Devices of the Ministry of Education & Shaanxi Key Lab of Information Photonic Technique, Collaborative Innovation Center of Suzhou Nano Science and Technology, School of Electronics & Information Engineering, Xi'an Jiaotong University, No. 28, Xianning West Road, Xi'an, 710049, China

^b Department of Applied Physics, Xi'an University of Technology, Yanxiang Road 58, Xi'an, 710054, China



ARTICLE INFO

Article history:

Received 23 July 2014

Received in revised form 17 October 2014

Accepted 3 November 2014

Available online 11 November 2014

Keywords:

Silicon groove

Chemical selective etching

Femtosecond laser

Laser microprocessing

ABSTRACT

Morphologies of high-aspect-ratio silicon grooves fabricated by using femtosecond laser irradiation and selective chemical etching of hydrofluoric acid (HF) were studied. Oxygen was deeply doped into silicon under femtosecond laser irradiation in air, and then the oxygen-doped regions were removed by HF etching to form high-aspect-ratio grooves. After HF etching, periodic nano-ripples which were induced in silicon by femtosecond laser were observed on the groove sidewalls. The ripple orientation was perpendicular or parallel to the laser propagation direction (z direction), which depended on the relative direction between the laser polarization direction and the scanning direction. The formation of nano-ripples with orientations perpendicular to z direction could be attributed to the standing wave generated by the interference of the incident light and the reflected light in z direction. The formation of nano-ripples with orientations parallel to z direction could be attributed to the formation of self-organized periodic nanoplates (bulk nanogratings) induced by femtosecond laser inside silicon. Materials in the tail portion of laser-induced oxygen doping (LIOD) regions were difficult to be etched by HF solution due to low oxygen concentration. The specimen was etched further in KOH solution to remove remaining materials in LIOD regions and all-silicon grooves were fabricated.

© 2014 Elsevier B.V. All rights reserved.

1. Introduction

High-aspect-ratio (HAR) silicon grooves are important for micro-electro-mechanical systems (MEMS), microfluidic devices and so on [1–9]. In MEMS, HAR grooves are basic structures in the trench isolation CMOS technology, which makes it possible to integrate MEMS and electronics on one chip [1–3]. Microgrooves are more widely used in micro-fluidic devices as microchannels or microchambers [4]. Many devices based on microgrooves such as microchemical reactors [5,6], microsensors [7], and so on have been demonstrated. In addition, heat sinks with microgroove array on back side show excellent thermal control capability [8]. Silicon microgroove grating is also an important element for terahertz radiation [9].

Many techniques have been carried out to fabricate HAR microstructures. Anisotropic wet etch is commonly employed for fabricating HAR silicon microstructures [10]. Alkaline solutions such as the potassium hydroxide (KOH) solution and

tetramethylammonium hydroxide (TMAH) were usually used as etchants for wet etching of silicon. However, only silicon wafers with specific orientations such as (1 1 0) could be adopted for fabricating HAR grooves by using anisotropic wet etch. For the latest two decades, the workhorse for HAR microstructures fabrication has been the deep reactive-ion etching (DRIE). DRIE is a highly anisotropic dry etching process. It can be applied to create HAR grooves and other structures with aspect ratios over 10:1 but usually below 40:1 [11,12]. However, DRIE requires expensive tooling. It is also a complex technology because its overall etching rate depends on many parameters. In addition, silicon grooves have also been fabricated by laser ablation in gas and liquid environments [13,14]. During the process, however, the debris generated by laser ablation blocked the energy delivery in deeper region of silicon and hampered the increase in the groove depth and aspect ratio. Recently, our group found femtosecond laser could induce structure changes including buried microchannels formation and element change inside silicon [15–17]. When the silicon was irradiated by femtosecond laser in air, oxygen was incorporated into the silicon simultaneously. The doping depth of oxygen could be more than 200 μm [15]. Further, the laser-induced oxygen doping (LIOD) regions were selectively etched by hydrofluoric acid (HF) to form

* Corresponding author. Tel.: +86 029 82663485.

E-mail address: jinhaisi@mail.xjtu.edu.cn (J. Si).

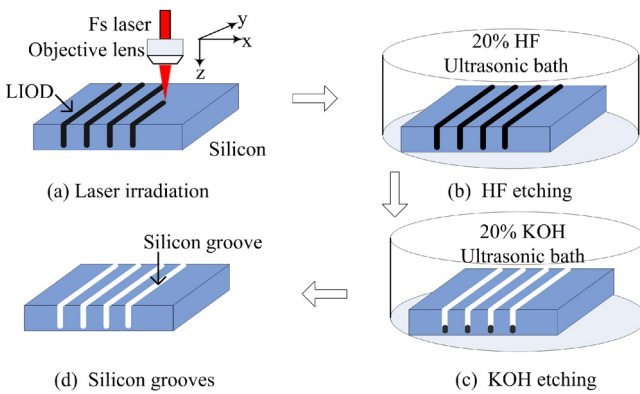


Fig. 1. Schematic diagram of microgrooves fabrication.

HAR grooves. Grooves with aspect ratio of 44 have been attained by using this method [18,19]. However, the surface morphology of grooves is still unknown.

Surface morphology of grooves is an important character for applications. Usually, smooth groove surface is expected for applications. On the other hand, textured surface with micro- and nano-structures could diversify functions of the microgrooves. It is well known that the micro- and nano-structures significantly influence the surface wettability. By patterning micro- and nano-structures on microchannel sidewalls, the liquid flow in microchannels could be controlled [20,21]. Surface microstructures on microchannel sidewalls were also applied to capture cells in microchannels [22]. In addition, nanostructured surfaces have been widely applied for surface enhanced Raman scattering (SERS) spectroscopy measurements [23,24].

In this paper, we studied the morphology of HAR silicon grooves fabricated by using femtosecond laser irradiation and selective chemical etching. Silicon wafers were firstly irradiated by femtosecond laser to form deep oxygen-doped regions. Then materials in LIOD regions were etched by HF solution to form grooves. Periodic nano-ripples were found on the groove sidewalls. The periodic structures were induced by femtosecond laser in silicon prior to HF acid etching. The ripple orientation was perpendicular or parallel to the laser propagation direction (z direction), which depended on the relative direction between the laser polarization direction and the scanning direction. The ripple periods were about 120 nm and 140 nm, respectively. The formation of nano-ripples with orientations perpendicular to z direction could be attributed to the standing wave generated by the interference of the incident light and the reflected light in z direction. The formation of nano-ripples with orientations parallel to z direction could be attributed to the formation of self-organized periodic nanoplanes induced by femtosecond laser inside silicon. In addition, the tail portion of LIOD region was difficult to be etched by HF solution due to low oxygen concentration. After the specimen was etched further in KOH solution, the remaining materials in the tail portion of LIOD regions were completely removed and all-silicon grooves with an aspect ratio of 26 were fabricated. The dependence of silicon groove dimensions on the laser fluence was studied after KOH etching.

2. Experimental setup

The overall fabrication process for grooves in silicon wafers is schematically described in Fig. 1, which shows two principal steps: laser-induced oxygen doping in silicon and wet etching. The morphology and chemical compositions of the LIOD regions and the selectively etched grooves were characterized by a scanning electronic microscopy (SEM, FEI Quanta 250 FEG Serials) equipped with

an energy dispersive X-ray spectroscopy (EDS, TEAMTM Serials), respectively.

2.1. Femtosecond laser-induced oxygen doping

In our experiments, a 50-fs Ti:sapphire regenerative amplifier system (Libra-USP-HE, Coherent Inc.) was employed as light source, which outputs 1-kHz pulse trains with pulse energy of 4 mJ/pulse and central wavelength of 800 nm. The laser pulse fluence was controlled by a variable neutral density attenuator, and the access of laser beam was controlled by a mechanical shutter. The laser beam was focused normally onto the specimen by a $10\times$ objective lens (numerical aperture of 0.3, Nikon lens) to induce structure change in silicon. In experiments, the incident beam filled only about 70% of the input aperture of the objective lens. Hence, the effective numerical aperture of the objective lens was reduced to 0.2. The spot size at focus was estimated to be about 3.3 μm in diameter. Specimen was mounted on a computer controlled three dimensional (3D) xyz translation stage (ProScan IITM). The focal spot was set on the specimen surface. Laser polarization was set along x direction in horizontal plane.

A p-type silicon wafer with a thickness of 500 μm was used in experiments, which was (100) in the crystal orientation. Prior to laser irradiation, silicon wafers were cleaned in an ultrasonic acetone bath, followed by a methanol bath. Then the silicon specimen was mounted on a 3D translation stage and LIOD patterns were formed by scanning the focused laser beam over silicon surfaces. The scanning direction was along the x axis or y axis. The scan length was 800 μm for each scanning line, and the separation distance was set at 80 μm to avoid the overlap between two adjacent scanning lines. After laser treating, the specimen surface perpendicular to the scanning direction was polished with water proof abrasive papers to a random position to observe LIOD and groove morphologies from side view. The polished specimen was ultrasonically cleaned by acetone, alcohol and deionized water for 15 min each before characterization.

2.2. Wet etching

For fabricating silicon grooves, the laser treated silicon wafers were immersed in 20 wt% HF acid solution for 60 min in an ultrasonic cleaner to remove materials in the LIOD regions. The temperature of the ambient water rose from 20 °C to about 40 °C due to ultrasonic shocking process. After HF etching, silicon specimen was then etched in 20 wt% KOH solution in an ultrasonic cleaner for 20 min.

3. Experimental results and discussion

3.1. Grooves fabricated by HF solution etching

Fig. 2 shows results before and after HF etching of specimen. The specimen was irradiated by the femtosecond pulse at the laser fluence of 409 J/cm² and the scan velocity of 5 $\mu\text{m}/\text{s}$. This scan velocity led to the accumulation of 660 pulses per spot. The scanning direction was along y axis (perpendicular to the laser polarization). As shown in Fig. 2a, laser-induced structure change regions were formed in silicon after femtosecond laser irradiation. According to the EDS analysis, we found that LIOD occurred in laser-induced structure change regions. The average depth of LIOD region along z direction was about 250 μm . The atomic percentage of oxygen decreased from 36% at the top to 0% at the end of LIOD region. After 60 min HF solution etching, materials in LIOD regions were selectively removed and grooves were formed as shown in Fig. 2b. The average groove depth and width were about 182 μm and 8.5 μm , respectively. The groove aspect ratio was about 21.4.

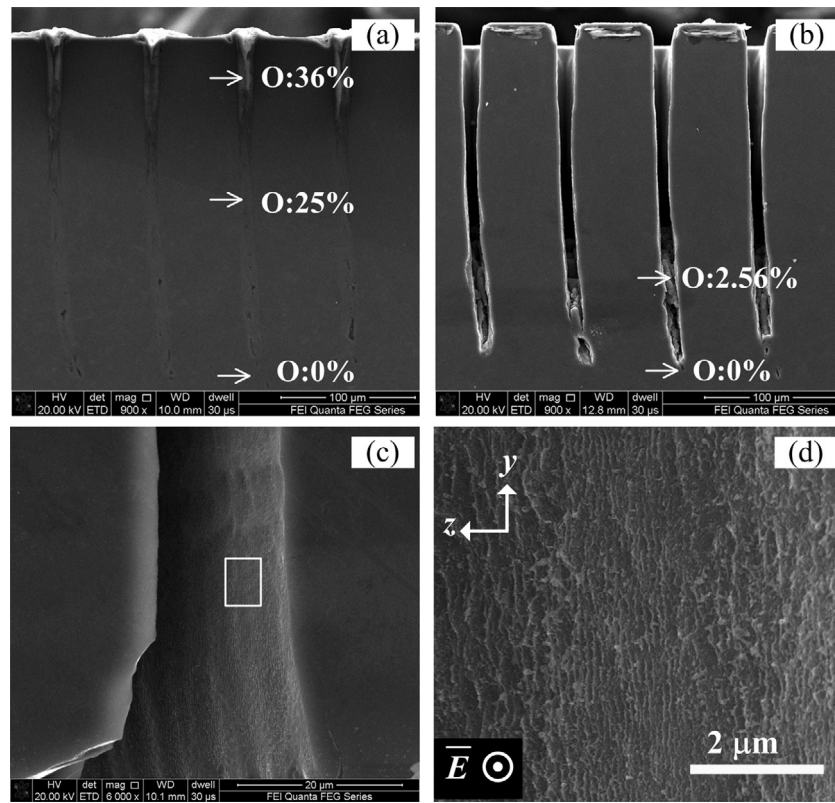


Fig. 2. Cross-sectional SEM images of LIOD regions (a) before and (b) after 20 wt% HF acid etching. The etching time was 60 min. (c) is the SEM image of the groove sidewall in (b), and (d) shows the detailed morphology of the marked area in (c).

In addition, the tail portion of LIOD regions was not completely removed by HF etching. The unreacted tail portion remained as debris on the groove bottoms. The length of remaining LIOD portion was about 70 μm. The atomic percentage of oxygen in debris at the top of the unreacted LIOD portion was measured to be less than 2.56%. The remaining debris on the groove bottoms was difficult to be removed by HF solution. According to our previous research, the reason that silicon irradiated by femtosecond laser could react with HF acid is because silicon oxide was formed [18,19]. The low oxygen concentration in remaining debris may make the reaction between debris and HF acid solution very slow. Other method should be applied for removing debris.

On the other side, the LIOD regions are not perpendicular to the original surface all over but show a curve in the deeper region. This could be explained as follows: the LIOD region was formed from top to down under laser irradiation of pulse by pulse. It is reasonable to suppose that the refractive index of LIOD region was different with that of raw silicon. Reflection of incident light would occur on the interface of LIOD region and raw silicon. When very slight asymmetry occurred to the LIOD regions formed by the firstly arriving pulses (for example laser was slightly obliquely incident), the propagation direction of the succeeding pulses would be changed and resulted in a slightly oblique LIOD segment in deeper region. The oblique LIOD segment would increase the deviation angle of the propagation direction of succeeding pulses from incident direction further. With the accumulation of pulses in silicon, the LIOD segments would extend to deeper and deeper region in silicon, which resulted in a LIOD region formation. The oblique angle of LIOD segment would also increase with the increase in depth. When very deep LIOD region was formed in silicon, even very slightly oblique of the top part may result in a curve shape in the deeper region.

Fig. 2c and d illustrates morphologies of groove sidewalls. It is interesting to observe that periodic nano-ripples with a periodicity

of about 120 nm were formed on groove sidewalls. Orientation of nano-ripples was along y direction, which was perpendicular to the laser propagation direction and the laser polarization. The nano-ripple structures should be induced in silicon by femtosecond laser prior to HF etching. After materials in LIOD region were removed, nano-ripples were observed on groove sidewalls.

Then the influence of the relative direction of the laser polarization and the scanning direction on the nano-ripple structures was studied. The grooves were fabricated by using the same parameters as that used for the above specimen, except that the scanning direction was along x axis (parallel to the laser polarization direction). The results were shown in Fig. 3. We can see that the nano-ripple

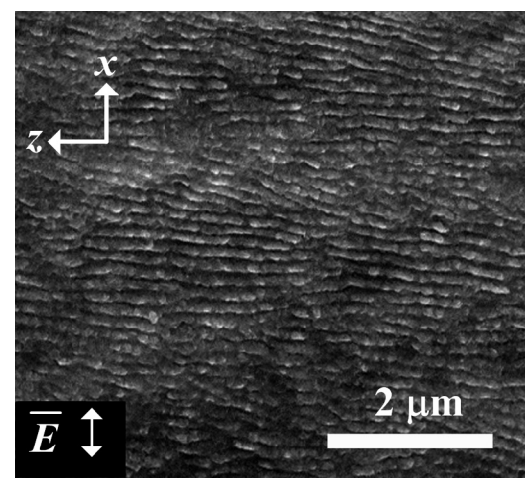


Fig. 3. The SEM image of the groove sidewall for the scanning direction was parallel to laser polarization direction (x axis).

orientation was parallel to the laser propagation direction (z direction) but still perpendicular to the laser polarization direction. The periodicity was about 140 nm, which was a little different with that in Fig. 2.

The orientation features of the nano-ripples on silicon groove sidewalls were summarized as follows: when the scanning direction was perpendicular to the laser polarization, the nano-ripple orientation was perpendicular to z direction; when the scanning direction was parallel to the laser polarization, the nano-ripple orientation was parallel to z direction. Nano-ripples formed on materials surface or inside materials have been reported widely [25–28]. Until now, only surface nano-ripples were observed on silicon [29–31]. The interference of incident light and surface plasma wave has been widely adopted to clarify the formation of the surface nano-ripples on silicon [29–31]. However, there has been few report concerning nano-ripples on sidewalls of holes or grooves induced by femtosecond laser irradiation. Weck and Khuat reported on the nano-ripples structures induced by femtosecond laser on the hole sidewalls in copper [32] and SiC [33], respectively. In our experiments, the relative directions of nano-ripple orientations with respect to the laser polarization direction and the propagation direction were the same as in their reports. In Refs. [32] and [33], the formations of nano-ripples were attributed to the interference effect.

We attributed the formation of nano-ripples on silicon grooves with different orientations to two different mechanisms. The formation of nano-ripples with orientation perpendicular to z direction (with 120-nm periodicity) could be attributed to the standing wave generated due to the interference between the incident light and the reflected light. The orientation of this type of nano-ripples was perpendicular to the laser propagation direction and had no dependence on laser polarization direction [33].

The nano-ripples on silicon grooves with orientation parallel to z direction (with 140-nm periodicity) could be attributed to the formation of self-organized periodic nanoplates induced by femtosecond laser inside silicon. It has been known that self-organized periodic nanoplates (also known as bulk nanogratings) could be induced inside fused silica by femtosecond laser irradiation [25,26]. The formation of self-organized periodic nanoplates was attributed to the interference between the incident light and the plasma waves [25,28]. More recently, a spherical nanoplasmas model was applied for describing the evolution of the periodic nanoplates. However, arguments on their formation still exist. The normal of periodic nanoplates was parallel to the laser polarization but perpendicular to the laser propagation direction. These self-organized periodic nanoplates extended over the full depth of the laser-modified region [26]. Self-organized periodic nanoplates may also be induced in silicon by femtosecond laser irradiation. When the scanning direction was parallel to the laser polarization, the normal of formed periodic nanoplates was along the scanning direction. After the LiOD regions were etched, nano-ripples were observed on the groove sidewalls as projections of nanoplates. The two mechanisms of nano-ripples formation coexisted. When the scanning direction was perpendicular to the laser polarization, projections of nanoplates on groove sidewall were just a plane and resulted in no periodic ripples on groove sidewalls. In this case, the nano-ripples formed by the standing wave could be shown on groove sidewalls. The superposition of these two mechanisms could be also applied for explaining results of the laser polarization dependence of the nano-ripples in Refs. [32] and [33].

For the two types of nano-ripples, the periodicities were $\lambda_0/(2n)$, where λ_0 and n were the laser wavelength in vacuum and refractive index of medium [26,33]. The refractive indexes n were calculated to be about 3.0, which was smaller than the silicon refractive index of 3.7 at 800 nm. The decrease of n could be attributed to the formation of plasma in silicon induced by femtosecond laser [25]. The

periodicities of nano-ripples observed on silicon groove sidewalls were smaller than that on SiC hole sidewalls. This may be due to larger refractive index of silicon compared with SiC.

3.2. KOH solution etching

To remove the debris on the groove bottoms, the specimen used in Fig. 2(b) was further immersed in 20% KOH solution with an

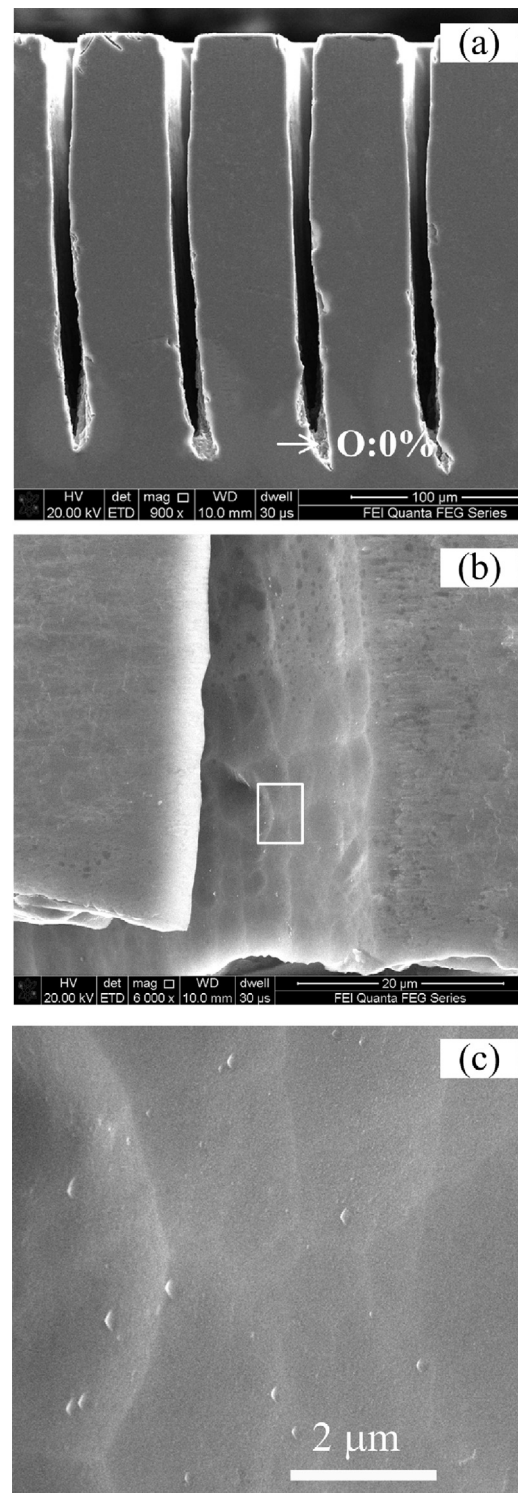
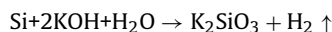


Fig. 4. (a) Cross-sectional and (b) sidewall SEM images of silicon grooves after 20 wt% KOH etching for the specimen in Fig. 2(b). The etching time was 20 min. (c) Detailed morphology of the marked area in (b).

ultrasonic bath. Fig. 4 shows the results that the specimen was etched for 20 min in KOH solution. As shown in Fig. 4a, the debris on the groove bottoms was removed completely and the average groove depth and width were increased to 256 μm and 9.8 μm , respectively. The groove aspect ratio was about 26. In addition, according to the EDS analysis, no oxides on the groove were detected and all-silicon groove were formed. Fig. 4b and c shows the morphologies of the groove sidewalls. Ripples on groove sidewalls were removed and shallow pits with smooth inner surface appeared on groove sidewalls. Although the sidewall surface was rough, it may be improved by optimizing KOH etching parameters.

The etching of debris by KOH solution was due to that the KOH could react with silicon. However, HF could only etch the silicon oxide. The pits formation was perhaps due to the anisotropic etching of KOH to silicon. The related reactive chemical equation can be expressed as follows:



In addition, we studied the dependences of groove dimensions on irradiation laser fluence. The results are shown in Fig. 5. The laser scan velocity was set at 5 $\mu\text{m}/\text{s}$ (660 pulses per spot). The specimen was etched successively by 20 wt% HF acid for 60 min and then 20 wt% KOH solutions for 20 min, respectively. When the laser fluence increased from 58 J/cm^2 to 409 J/cm^2 , groove depths increased from 75 to 256 μm , while groove widths increased from 6.0 to 9.8 μm . The groove aspect ratio increased with the increase in the laser fluence and reached about 26 at a laser fluence of 409 J/cm^2 . The increase of aspect ratio was unsaturated at the

maximal laser fluence of 409 J/cm^2 in Fig. 5. The formation of the HAR grooves could be attributed to that self-trapped filament of femtosecond laser occurred in the LIOD region [18]. With the further increase in the laser fluence, more nonlinear optical processes such as multiphoton absorption could be excited and disturbed the formation of filament in deeper region. Hence the filament length could not increase further with the increase in laser fluence, and the aspect ratio increase perhaps saturated at higher laser fluence.

4. Conclusion

In conclusion, we studied morphologies of grooves fabricated by femtosecond laser irradiation in air and selective chemical etching of HF acid. It was found that nano-ripples with orientations perpendicular and parallel to laser propagation direction were formed on the groove sidewalls. The formation of these two types of nano-ripples could be attributed to the interference of the incident light and the reflected light in z direction, and the formation of self-organized periodic nanoplates induced by femtosecond laser inside silicon, respectively. By using KOH etching further, remaining debris in LIOD regions was completely removed, which was difficult to be removed by HF acid, and all-silicon grooves were fabricated. In addition, nano-ripple structures on groove sidewalls were removed and shallow pits with smooth inner surface appeared.

The authors gratefully acknowledge the financial support for this work provided by the National Basic Research Program of China (973 Program) under Grant no. 2012CB921804, the National Natural Science Foundation of China (NSFC) under the Grant nos. 11204236 and 61308006, and Opened Fund of the State Key Laboratory on Integrated Optoelectronics No. IOSKL2012KF. The authors also sincerely thank Ms. Dai at International Center for Dielectric Research (ICDR) in Xi'an Jiaotong University for the support of SEM and EDS measurements.

References

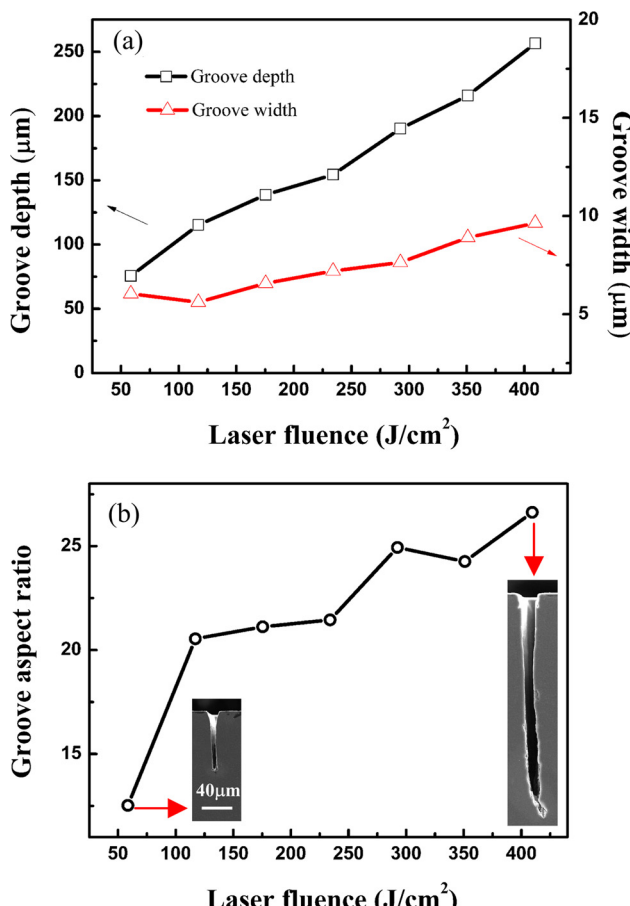


Fig. 5. (a) Depths, widths, and (b) aspect ratios of grooves versus femtosecond laser fluences. The grooves were fabricated by using femtosecond laser irradiation and then etched successively by 20 wt% HF for 60 min and 20 wt% KOH for 20 min.

- [1] W. Noell, P.A. Clerc, L. Dellmann, B. Guldmann, H.P. Herzig, O. Manzardo, C.R. Marxer, K.J. Weible, R. Dandliker, N. de Rooij, IEEE J. Sel. Top. Quant. Electron. 8 (2002) 148.
- [2] E. Sarajlic, M.J. de Boer, H.V. Jansen, N. Arnal, M. Puech, G. Krijnen, M. Elwenspoek, J. Micromech. Microeng. 14 (2004), S70.
- [3] G.K. Fedder, R.T. Howe, T. Liu, E.P. Quevy, Proc. IEEE 96 (2008) 306.
- [4] S. Ota, H. Suzuki, S. Takeuchi, Lab Chip 11 (2011) 2485.
- [5] K.F. Jensen, Mat. Res. Soc. Bull. 31 (2006) 101.
- [6] T.R. Henriksen, J.L. Olsen, P. Vesborg, I. Chorkendorff, O. Hansen, Rev. Sci. Instrum. 80 (2009) 124101.
- [7] V. Martini, S. Bernardini, M. Bendahan, K. Aguir, P. Perrier, I. Graur, Sens. Actuators B—Chem. 170 (2012) 45.
- [8] T.L. Chen, S.V. Garimella, J. Int. Heat Mass Transf. 54 (2011) 3179.
- [9] M. Kuttge, H. Kurz, J.G. Rivas, J.A. Sánchez-Gil, P.H. Bolívar, J. Appl. Phys. 101 (2007) 023707.
- [10] V.K. Dwivedi, R. Gopal, S. Ahmad, J. Microelectron. 31 (2000) 405.
- [11] C. Gu, H. Xu, T. Zhang, J. Micromech. Microeng. 19 (2009) 065011.
- [12] P. Dixit, J. Miao, J. Electrochem. Soc. 153 (2006), G552.
- [13] T. Crawford, A. Borowiec, H.K. Haugen, Appl. Phys. A—Mater. 80 (2005) 1717.
- [14] D.H. Kam, L. Shah, J. Mazumder, J. Micromech. Microeng. 21 (2011) 045027.
- [15] Y. Ma, H. Shi, J. Si, T. Chen, F. Yan, F. Chen, X. Hou, Opt. Commun. 285 (2012) 140.
- [16] T. Chen, J. Si, X. Hou, S. Kanehira, K. Miura, K. Hirao, Appl. Phys. Lett. 93 (2008) 051112.
- [17] C. Li, X. Shi, J. Si, F. Chen, T. Chen, Y. Zhang, X. Hou, Appl. Phys. B 98 (2010) 377.
- [18] A. Pan, J.H. Si, T. Chen, Y.C. Ma, F. Chen, X. Hou, Opt. Express 21 (2013) 16657.
- [19] Y.C. Ma, A. Pan, J.H. Si, T. Chen, F. Chen, X. Hou, Appl. Surf. Sci. 284 (2013) 372.
- [20] C. Lee, C.J. Kim, Langmuir 25 (2009) 12812.
- [21] T. Yamada, C. Hong, O.J. Gregory, M. Faghri, Microfluid. Nanofluid. 11 (2011) 45.
- [22] A. Khademhosseini, J. Yeh, S. Jon, G. Eng, K.Y. Suh, J.A. Burdick, R. Langer, Lab Chip 4 (2004) 425.
- [23] C.H. Lin, L. Jiang, Y.H. Chai, H. Xiao, S.J. Chen, H.L. Tsai, Opt. Express 17 (2009) 21581.
- [24] B.B. Xu, Z.C. Ma, H. Wang, X.Q. Liu, Y.L. Zhang, X.L. Zhang, R. Zhang, H.B. Jiang, H.B. Sun, Electrophoresis 32 (2011) 3378.

- [25] Y. Shimotsuma, P.G. Kazansky, J.R. Qiu, K. Hirao, Phys. Rev. Lett. 91 (2003) 247405.
- [26] V.R. Bhardwaj, E. Simova, P.P. Rajeev, C. Hnatovsky, R.S. Taylor, D.M. Rayner, P.B. Corkum, Phys. Rev. Lett. 96 (2006) 057404.
- [27] G. Miyaji, K. Miyazaki, K. Zhang, T. Yoshifiji, J. Fujita, Opt. Express 20 (2012) 14848.
- [28] M. Huang, F.L. Zhao, Y. Cheng, N.S. Xu, Z.Z. Xu, Acs Nano 3 (2009) 4062.
- [29] W. Han, L. Jian, X. Li, P. Liu, L. Xu, Y. Lu, Opt. Express 21 (2013) 15505.
- [30] M. Straub, M. Afshar, D. Feili, H. Seidel, K. Koning, Opt. Lett. 37 (2012) 190.
- [31] T. Tomita, Y. Fukumori, K. Kinoshita, S. Matsuo, S. Hashimoto, Appl. Phys. Lett. 92 (2008) 013104.
- [32] A. Weck, T. Crawford, D.S. Wilkinson, H.K. Haugen, J.S. Preston, Appl. Phys. A—Mater. 89 (2007) 1001.
- [33] V. Khuat, T. Chen, B. Gao, J. Si, Y. Ma, X. Hou, Appl. Phys. Lett. 104 (2014) 241907.